Title	Electroosmotic flow of a viscoplastic material through a slit channel with walls of arbitrary zeta potential
Author(s)	Ng, CO; Qi, C
Citation	Physics of Fluids, 2013, v. 25 n. 10, p. article no. 103102
Issued Date	2013
URL	http://hdl.handle.net/10722/192558
Rights	Physics of Fluids. Copyright © American Institute of Physics.

Electroosmotic flow of a viscoplastic material through a slit channel with walls of arbitrary zeta potential

Chiu-On Ng and Cheng Qi

Citation: Physics of Fluids (1994-present) **25**, 103102 (2013); doi: 10.1063/1.4825368
View online: http://dx.doi.org/10.1063/1.4825368
View Table of Contents: http://scitation.aip.org/content/aip/journal/pof2/25/10?ver=pdfcov
Published by the AIP Publishing

PHYSICS OF FLUIDS **25**, 103102 (2013)

Electroosmotic flow of a viscoplastic material through a slit channel with walls of arbitrary zeta potential

Chiu-On Ng[a] and Cheng Qi
Department of Mechanical Engineering, The University of Hong Kong, Pokfulam Road, Hong Kong

(Received 6 May 2013; accepted 3 October 2013; published online 22 October 2013)

Electroosmotic (EO) flow is known to have a nearly uniform velocity profile, but such a plug-flow velocity can be considerably diminished if the fluid is a viscoplastic material having a yield stress. This paper aims to investigate the reduction of EO velocity (also known as Smoluchowski slip velocity) due to a yield stress as a function of the material rheological parameters and the zeta potential. Three rheological models are considered: Casson, Herschel–Bulkley, and Bingham fluids. In the absence of pressure forcing and without the Debye–Hückel approximation, the problems of EO flow of these materials in a slit channel with walls uniformly charged with an arbitrary zeta potential are analytically solved. Analytical expressions are deduced for the reduced Smoluchowski velocity under the limiting conditions of very small and very large zeta potentials. It is shown that qualitatively different asymptotic behaviors will be exhibited by materials of different models. © *2013 AIP Publishing LLC*. [http://dx.doi.org/10.1063/1.4825368]

I. INTRODUCTION

During the recent years there has been a growing interest in the study of non-Newtonian fluid flow in microchannels. Such need arises from the fact that many fluids to be analyzed using the so-called lab-on-a-chip devices are complex fluids, which can be biofluids, colloidal solutions, solutions of high polymers, and suspensions. Such fluids are often classified according to their rheological behaviors as shear thinning/thickening, viscoelastic, viscoplastic, structuralized fluids, and so on.

On a microscale, the hydrodynamics can become more intriguing when the fluid is a generalized Newtonian material, of which the viscosity may change as a function of the shear rate. In the absence of inertia, a low-Reynolds-number flow is so much affected by the viscous force that the rheology of the material can play a central role in determining the flow behaviors. Microhydrodynamics of complex fluids[1] is an emerging topic drawing attention from both applied and basic research communities.

Flow in a microchannel can be driven by pressure gradient, electrokinetics, or a combination of both. Flow that happens under an applied electric field is called electroosmotic (EO) flow. It results from the interaction of the electric field and mobile ions in the electric double layer (EDL) formed on a charged surface. The electric double layer comprises an inner Stern layer, where counterions (ions of opposite charge to that of the surface) are firmly attached to the surface, and an outer diffuse layer, where counterions outnumber coions and form a charged atmosphere shielding the bulk solution from the charged surface. The electric potential at the shear plane, where the no-slip boundary condition is assumed to apply, is called zeta potential. The net charge density drops off exponentially through the diffuse layer, asymptotically approaching zero far from the surface. The length scale that defines the exponential drop-off of the net charge density is known as the Debye shielding length, which is also a measure of the thickness of the EDL.

[a] Author to whom correspondence should be addressed. Electronic mail: cong@hku.hk.

The fact that EO velocity does not depend on the channel size is an advantage often harvested by applications that require flow in ultrafine channels. Pure EO flow is also known to be a nearly plug-like flow when the EDL is much thinner than the lateral dimension of the channel. Such plug-like EO flow can be visualized as flow resulting from a boundary slip, where the slip velocity is known as the Smoluchowski slip velocity.[2] It is often that analysis of EO flow in a channel of complex geometry is simplified using the Smoluchowski slip velocity as the boundary condition, thereby avoiding the need to solve the momentum equation with the Lorentz body force. This approach works, however, only for Newtonian EO flows. When the fluid is non-Newtonian, nonlinear interaction between mechanical and electric forcings will make linear superposition of solutions due to individual forcings illegitimate.

EO flow of a non-Newtonian fluid was not theoretically investigated until recently. Motivated to study biofluids in micro-systems, Das and Chakraborty[3] and Zimmerman *et al.*[4] pioneered to develop theories on non-Newtonian electrokinetic flow and transport in microchannels. To this date, the power-law model has been the most chosen rheological model for studies on EO flow of non-Newtonian fluids in microchannels. Examples are: Chakraborty,[5] Berli and Olivares,[6] Zhao *et al.*,[7] Bharti *et al.*,[8] Olivares *et al.*,[9] Tang *et al.*,[10] Zhao and Yang,[11–13] Berli,[14] Vasu and De,[15,16] Babaie *et al.*,[17] Hadigol *et al.*,[18] Sadeghi *et al.*,[19] Cho *et al.*,[20,21] Shamshiri *et al.*,[22] Vakili *et al.*,[23] and so on. The power-law model is a relatively simple two-parameter model, where the shear-thinning, Newtonian, or shear-thickening behaviors are conveniently modeled by setting the flow index to be less than, equal to, or larger than 1, respectively.

While the power-law model can be used to describe pseudo-plastic or dilatant behaviors, the viscoplastic characters cannot be described unless a yield stress is introduced. A material with a yield stress either does not flow, or flows like a rigid body when the stress is smaller in magnitude than the yield stress. Viscoplastic materials with a yield stress have been reviewed in detail by Bird *et al.*[24] They reviewed several viscoplastic models, which can be used to describe many yield-stress materials frequently encountered in industrial problems, including pastes, slurries, and suspensions. The magnitude of yield stress varies in different fluids, for example, 4 mPa for a normal blood with 40% hematocrit[25] and 7 to 11 Pa for a mineral suspension with 52 wt. % solids.[26] There exist, however, only a limited number of works in the literature[6,27–29] which have considered EO flow of fluids with a yield stress. How the yield stress will affect an EO flow has remained largely unknown thus far. This is the motivation for the present study.

This work aims to develop analytical solutions for EO flow of a yield-stress material through a parallel-plate channel, of which the walls are uniformly charged with an arbitrary zeta potential. Three types of viscoplastic materials, viz. Casson fluid, Herschel–Bulkley fluid, and Bingham plastic,[24] are considered. The specific objectives are as follows, which should distinguish our work from those in the literature.

The primary objective to look into the decreasing effect due to a yield stress on the EO velocity, where the yield-stress effect may change qualitatively depending on the viscoplastic model. Analytical expressions are deduced for velocity profiles for the three types of materials. Each velocity profile consists of a sheared region, where the yield stress is exceeded, and an unsheared region, where the stress is below the yield stress. The yield surface, which is the interface separating the sheared and unsheared regions, is located within the near-wall EDL. Therefore, it is the uniform velocity in the unsheared region that dominates the velocity profile. This uniform velocity profile, resulting from a yield stress, looks similar to the classical plug-like EO velocity profile without a yield stress. However, the former is a result of interaction between rheological properties of fluid and electric forcing, and is therefore subject to more controlling factors than the latter.

The yield-stress effect can also change dramatically depending on the electric forcing. Hence, another objective of this study is to examine EO flow of a yield-stress material when the zeta potential can be large or small. The Debye–Hückel approximation, which follows from the assumption of small electric potential and is often used to linearize the Poisson–Boltzmann equation, is not adopted in this work. Without the Debye–Hückel approximation, our model can handle both limits of small and large zeta potentials. Zeta potential is a very crucial factor in the present problem, as it will determine the stress distribution, which will in turn determine the flow in the sheared and unsheared regions. Existing studies that have considered EO flow of non-Newtonian fluids under a large zeta

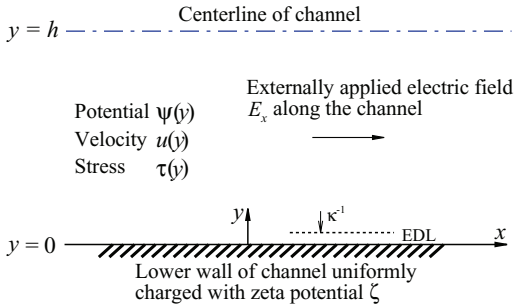

FIG. 1. Definition sketch of the problem: one-dimensional flow of velocity $u(y)$ and shear stress $\tau(y)$, forced by an externally applied electric field E_x, through a slit channel of height $2h$. The wall is uniformly charged with a constant zeta potential ζ, giving rise to static electric potential $\psi(y)$. The electric double layer (EDL) is much thinner than the channel height $\kappa h \gg 1$.

potential include Bharti *et al.*,[8] Zhao and Yang,[12,30] Vasu and De,[16] Babaie *et al.*,[17] Vakili *et al.*,[23] and so on. Yield stress is, however, not considered in these studies.

Our problem is described in further detail in Sec. II. Strictly one-dimensional steady EO flow without pressure forcing is considered. For a simple flat surface, the nonlinear Poisson–Boltzmann equation for the electric potential has the classical Gouy–Chapman solution. The Cauchy momentum equation can then be readily solved for the stress as a function of the zeta potential. These details are given in Sec. III. The known stress distribution allows the location of the yield surface to be found as a function of the yield stress and the zeta potential, which is detailed in Sec. IV. In Secs. V–VII, the velocity profiles for Casson, Herschel–Bulkley, and Bingham fluids are derived. The plug-flow velocities, which can be regarded as reduced Smoluchowski velocities, are expressed as analytically as possible. The analytical limits for the velocities under small and large zeta potentials are deduced as well. We then examine in Sec. VIII, with numerical results, how the plug-flow velocity is affected by the yield stress and the zeta potential for each of the three viscoplastic models. It will be shown that the dependence of the flow on the yield stress changes as a function of the zeta potential, and comparisons will be made for the effects of yield stress among different materials.

II. PROBLEM DESCRIPTION

Consider EO flow of a viscoplastic material through a slit channel bounded by two parallel flat plates, which are at a distance of $2h$ apart. The surfaces of the two plates are uniformly charged with the same zeta potential ζ. Figure 1 shows a definition sketch of our problem. The electric potential ψ and the flow are both symmetrical about the centerline of the channel. Hence, it suffices for us to limit our analysis to the lower half of the channel: $0 \le y \le h$, where the transverse coordinate y is the distance from the lower wall of the channel. The flow is purely one-dimensional, forced by an externally applied steady electric field E_x in the x-direction. There is no pressure gradient, whether applied or induced, in the flow. Gravity effect is also ignored. The fluid is assumed to be a homogeneous material with constant rheological parameters, and a constant dielectric permittivity ϵ. The flow being steady, laminar, and fully developed, we denote the axial velocity and the shear stress by $u_x = u(y)$ and $\tau_{xy} = \tau(y)$, respectively. We assume that the electric double layer that is formed near the wall is much thinner than the channel height. The electric potential is therefore virtually zero in the bulk fluid.

III. ELECTRIC POTENTIAL AND STRESS DISTRIBUTIONS

In the absence of pressure gradient and gravity effect, the Cauchy momentum equation for flow driven by an electric body force reads as follows:

$$0 = \frac{d\tau}{dy} + \rho_e E_x, \tag{1}$$

where E_x is the applied electric field, and $\rho_e = \rho_e(y)$ is the free charge density in the EDL.

By electrostatics, the electric potential $\psi(y)$ in the EDL is related to the net charge density ρ_e, given by the Poisson equation

$$\frac{d^2\psi}{dy^2} = -\frac{\rho_e}{\epsilon}, \tag{2}$$

where ϵ is the dielectric permittivity of the liquid electrolyte. With the further assumptions of a Boltzmann distribution for the ions in the EDL and a symmetric electrolyte solution, ρ_e is given by

$$\rho_e = -2zen_\infty \sinh\left(\frac{ze\psi}{k_BT}\right), \tag{3}$$

where e is the fundamental charge, z is the valence of the ions, n_∞ is the bulk concentration, k_B is the Boltzmann constant, and T is the absolute temperature. Combining Eqs. (2) and (3) forms the Poisson–Boltzmann equation:

$$\frac{d^2\psi}{dy^2} = \frac{2zen_\infty}{\epsilon} \sinh\left(\frac{ze\psi}{k_BT}\right), \tag{4}$$

with the boundary conditions

$$\psi = 0 \qquad \text{at } y \to \infty, \tag{5}$$

$$\psi = \zeta \qquad \text{at } y = 0, \tag{6}$$

where $y \to \infty$ means a distance from the wall that is much larger than the EDL thickness (see below). The solution to Eqs. (4)–(6) is given by the well-known Gouy–Chapman solution

$$\hat{\psi}(\hat{y}) = \frac{1}{2\hat{\zeta}} \ln\left[\frac{1 + \tanh(\hat{\zeta})e^{-\hat{\kappa}\hat{y}}}{1 - \tanh(\hat{\zeta})e^{-\hat{\kappa}\hat{y}}}\right], \tag{7}$$

where $\hat{\psi} = \psi/\zeta$ is the normalized electric potential,

$$\hat{\zeta} = ze\zeta/(4k_BT) \tag{8}$$

is a non-dimensional parameter for the zeta potential, and

$$\hat{\kappa} = \kappa h, \qquad \hat{y} = y/h, \tag{9}$$

in which $\kappa = (2n_\infty z^2e^2/\epsilon k_BT)^{1/2}$ is termed the Debye parameter, the inverse of which is the Debye shielding length or the thickness of the EDL. The condition that the EDL is much thinner than the channel height amounts to the condition $\hat{\kappa} \gg 1$. For any $\hat{\zeta}$, the electric potential drops off exponentially with distance from the wall according to $\exp(-\hat{\kappa}\hat{y})$. One can find that $\hat{\psi}$ becomes practically negligible at a distance about 6 times the Debye length from the wall, $\hat{\kappa}\hat{y} > 6$. Also, the normalized potential $\hat{\psi}$ at any $\hat{\kappa}\hat{y} > 0$ decreases as $\hat{\zeta}$ increases.

With Eq. (2), and using the conditions that the stress and the electric potential gradient are zero at $\hat{y} = 1$, Eq. (1) can be readily integrated to give

$$\hat{\tau} = -\frac{1}{\hat{\kappa}}\frac{d\hat{\psi}}{d\hat{y}}, \tag{10}$$

where $\hat{\tau} = \tau/\tau_E$ is the non-dimensional shear stress that has been normalized by

$$\tau_E = -\epsilon\kappa\zeta E_x, \tag{11}$$

which is the wall stress under the limiting condition $\hat{\zeta} \ll 1$. Without loss of generality, we shall assume that τ_E is positive.

On substituting Eq. (7) into Eq. (10), the stress distribution is found to be

$$\hat{\tau}(\hat{y}) = \frac{\sinh(2\hat{\zeta})/(2\hat{\zeta})}{\cosh^2(\hat{\zeta})e^{\hat{\kappa}\hat{y}} - \sinh^2(\hat{\zeta})e^{-\hat{\kappa}\hat{y}}} \qquad 0 \le \hat{y} \le 1, \tag{12}$$

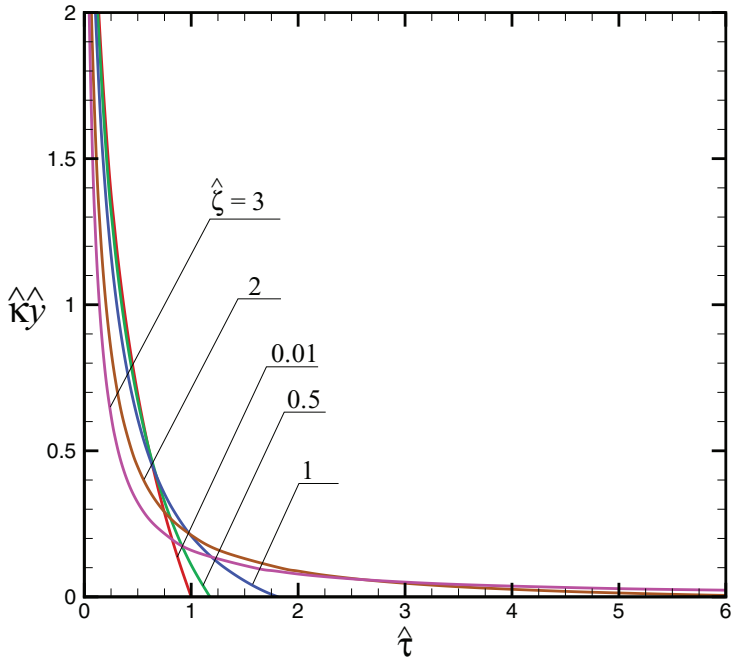

FIG. 2. Distribution of stress $\hat{\tau}$, given by Eq. (12), as a function of stretched coordinate $\hat{\kappa}\hat{y}$, and normalized zeta potential $\hat{\zeta}$.

which is applicable to any generalized Newtonian fluids. The stress at the wall is

$$\hat{\tau}_w = \hat{\tau}(0) = \frac{\sinh(2\hat{\zeta})}{2\hat{\zeta}}, \tag{13}$$

which is also the maximum stress in the entire distribution. The stress will decrease from the wall at a rate given by

$$\left.\frac{d\hat{\tau}}{d\hat{y}}\right|_{\hat{y}=0} = -\hat{\kappa}\frac{\sinh(4\hat{\zeta})}{4\hat{\zeta}}. \tag{14}$$

Increasing the zeta potential $\hat{\zeta}$ will not only exponentially increase the stress at the wall, but also exponentially increase the rate of drop-off of the stress from the wall. These effects are clearly seen in Fig. 2, which shows the normalized stress $\hat{\tau}$ as a function of the stretched coordinate $\hat{\kappa}\hat{y}$ for several values of $\hat{\zeta}$. Equation (12) can be rewritten as

$$\hat{\tau}(\hat{y}) = \frac{\tanh(\hat{\zeta})/\hat{\zeta}}{e^{\hat{\kappa}\hat{y}} - \tanh^2(\hat{\zeta})e^{-\hat{\kappa}\hat{y}}}, \tag{15}$$

and hence, at a sufficiently large $\hat{\kappa}\hat{y}$, the shear stress is proportional to $\tanh(\hat{\zeta})/\hat{\zeta}$, which is a monotonously decreasing function of a positive $\hat{\zeta}$. As a result, with a larger zeta potential, the shear stress is larger at the wall but smaller away from the wall. This explains why there is always an intersection between two curves in Fig. 2.

In the particular case of a Newtonian fluid, the stress is linearly proportional to the shear rate, $\tau = \mu du/dy$, where μ is the dynamic viscosity of the fluid. We may write

$$\hat{\tau} = \frac{1}{\hat{\kappa}}\frac{d\hat{u}}{d\hat{y}} \qquad \text{for Newtonian fluid,} \tag{16}$$

where $\hat{u} = u/u_s$ is the non-dimensional velocity that has been normalized by the Smoluchowski velocity for Newtonian fluid,

$$u_s = \tau_E/\mu\kappa = -\epsilon\zeta E_x/\mu. \tag{17}$$

From Eqs. (10) and (16), we readily get

$$\hat{u}(\hat{y}) = 1 - \hat{\psi}(\hat{y}) \qquad \text{for Newtonian fluid,} \tag{18}$$

on using the boundary conditions $\hat{u}(0) = 0$ and $\hat{\psi}(0) = 1$. Far outside the EDL, $\hat{y} \gg \hat{\kappa}^{-1}$, the potential is zero $\hat{\psi} = 0$, and therefore $\hat{u} = 1$. As is well known, the Smoluchowski velocity u_s is the plug flow velocity outside the EDL in the case of a Newtonian fluid, for large or small zeta potentials.

In the limiting case of a very small zeta potential, the following limits can be obtained from Eqs. (7) and (12):

$$\lim_{\hat{\zeta}\to 0} \hat{\psi}(\hat{y}) = e^{-\hat{\kappa}\hat{y}}, \qquad \lim_{\hat{\zeta}\to 0} \hat{\tau}(\hat{y}) = e^{-\hat{\kappa}\hat{y}}, \tag{19}$$

which agree with those derived under the Debye–Hückel approximation. In this limit, $\hat{\tau}_w = 1$, which confirms that τ_E given in Eq. (11) is indeed the wall stress under the limiting condition $\hat{\zeta} \ll 1$.

The zeta potential ζ that is available in practice is normally not larger than 200 mV, which corresponds to a normalized zeta potential $\hat{\zeta} = ze\zeta/(4k_BT) \approx 2z$ at a temperature of 25°C. Hence, for ions of valence one or two, the maximum normalized zeta potential that we may consider in practice should not exceed 5. To show the analytical trends, we shall, however, deduce and examine the asymptotic limits for very large zeta potential, $\hat{\zeta} \gg 1$, in Secs. IV–VIII. In the figures, only results for $\hat{\zeta} \le 5$ are presented.

IV. YIELDED AND UNYIELDED REGIONS

For a viscoplastic material with a normalized yield stress

$$\hat{\tau}_0 = \tau_0/\tau_E, \tag{20}$$

the material will not be set into motion by the applied electric field unless the maximum stress, which is the wall stress, exceeds the yield stress

$$\hat{\tau}_w = \frac{\sinh(2\hat{\zeta})}{2\hat{\zeta}} > \hat{\tau}_0. \tag{21}$$

When this condition is met, there exists a distance from the wall, $\hat{y} = \hat{y}_0$, at which the stress is equal to the yield stress: $\hat{\tau}(\hat{y}_0) = \hat{\tau}_0$. This defines the position of the yield surface. Let us call $\hat{y}_0$ the yield height, as it is also the height of the yielded region. Using Eq. (12), we may obtain after some algebra the yield height as

$$\hat{y}_0 = \hat{\kappa}^{-1} \ln\left[\frac{\tanh(\hat{\zeta})}{2\hat{\zeta}\,\hat{\tau}_0}\left(1 + \sqrt{1 + 4\hat{\tau}_0^2\hat{\zeta}^2}\right)\right]. \tag{22}$$

The yield height is zero, $\hat{y}_0 = 0$, when the fluid is on the threshold of motion: $\hat{\tau}_0 = \hat{\tau}_w$. The yield height will increase monotonically as the yield stress decreases from this threshold value. The upper limit is $\hat{y}_0 = 1$ when $\hat{\tau}_0 = 0$. In the limit of a small zeta potential, Eqs. (21) and (22) give

$$\lim_{\hat{\zeta}\to 0} \hat{\tau}_w = 1 > \hat{\tau}_0, \qquad \lim_{\hat{\zeta}\to 0} \hat{y}_0 = -\hat{\kappa}^{-1} \ln \hat{\tau}_0, \tag{23}$$

which agree with the those derived by Ng[29] based on the Debye–Hückel approximation. In the opposite limit of a very large zeta potential, we get from Eqs. (22) and (7)

$$\hat{y}_0 \to \frac{1}{2\hat{\zeta}\,\hat{\tau}_0\hat{\kappa}}, \quad \hat{\psi}(\hat{y}_0) \to \frac{1}{2\hat{\zeta}} \ln\left(4\hat{\zeta}\,\hat{\tau}_0\right) \qquad \text{for } \hat{\zeta} \gg 1, \text{ where } \hat{\tau}_0 = O(1). \tag{24}$$

When the wall stress exceeds the yield stress, the material will flow. The flow is divided into two regions: (i) the yielded (or sheared) region $0 \le \hat{y} < \hat{y}_0$, where $\hat{\tau} > \hat{\tau}_0$; (ii) the unyielded (or unsheared) region $\hat{y}_0 < \hat{y} \le 1$, where $\hat{\tau} < \hat{\tau}_0$. In the unsheared region, the shear rate is zero,

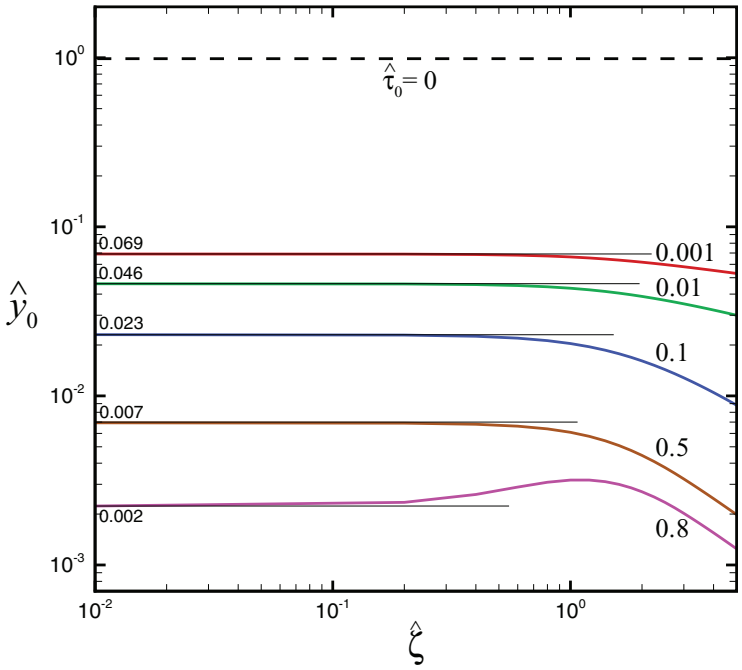

FIG. 3. Normalized yield height $\hat{y}_0$ as a function of the normalized zeta potential $\hat{\zeta}$ and normalized yield stress $\hat{\tau}_0$, where $\hat{\kappa} = 100$. The asymptotic limits for $\hat{\zeta} \to 0$, which are computed by Eq. (23), are shown on the left end of curves.

implying a constant velocity, and therefore a plug-like profile. For a yield stress $0 < \hat{\tau}_0 < \hat{\tau}_w$, the fluid flow will have a reduced height to develop its velocity before reaching a uniform flow at a definite point due to the presence of a yield surface. In sharp contrast, in the absence of a yield stress, the flow may develop its velocity across the entire EDL, on asymptotically approaching a uniform flow at the outer edge of the EDL ($\hat{\kappa}\hat{y} \gg 1$). The early attainment of uniform flow will cause a fluid with a yield stress to have a lower plug-flow velocity than its counterpart without a yield stress.

Figure 3 shows the normalized yield height $\hat{y}_0$ as a function of $\hat{\zeta}$ and $\hat{\tau}_0$. For a fixed yield stress $\hat{\tau}_0$, increasing the zeta potential $\hat{\zeta}$ will in general decrease the yield height, which can be understood with the effect of $\hat{\zeta}$ on the stress distribution as shown in Fig. 2. Remarkably, Fig. 3 reveals that the $\hat{\zeta} \to 0$ limit of the yield height can be practically attained when $\hat{\zeta} \leq O(1)$ for $\hat{\tau}_0 = O(0.1)$, and when $\hat{\zeta} \leq O(0.1)$ for $\hat{\tau}_0 = O(1)$. This suggests that the theoretical small-$\hat{\zeta}$ limit of $\hat{y}_0$, given in Eq. (23), remains practically applicable up to $\hat{\zeta} = O(1)$ or $\hat{\zeta} = O(0.1)$, depending on the yield stress. As a matter of course, increasing the yield stress will also decrease the yield height, as can be seen from Eqs. (23) and (24) for the small and large zeta potential limits. Hence, the yield height is reduced by either increasing $\hat{\zeta}$ for fixed $\hat{\tau}_0$ or increasing $\hat{\tau}_0$ for fixed $\hat{\zeta}$. As will be seen later, these two ways of decreasing the yield height will, however, lead to opposite effects on the plug-flow velocity in the unsheared region.

Let us develop in Secs. V–VII the velocity profiles for three specific viscoplastic materials.

V. CASSON FLUID

The model proposed by Casson[31] can be generalized into

$$\mu\dot{\gamma} = \begin{cases} \left[1 - \sqrt{\tau_0/|\tau|}\right]^2 \tau & \text{for } |\tau| > \tau_0 \\ 0 & \text{for } |\tau| \leq \tau_0 \end{cases}, \tag{25}$$

where τ is the stress tensor, $\dot{\gamma} = \nabla\mathbf{u} + (\nabla\mathbf{u})^T$ is the rate of deformation tensor, μ is the plastic viscosity, $\tau_0 \geq 0$ is the Casson yield stress, and

$$|\tau| = \sqrt{\tfrac{1}{2}\tau : \tau} \tag{26}$$

is the magnitude of the stress. The Casson model reduces to the Newtonian model when $\tau_0 = 0$.

Under simple shear, the Casson constitutive equation, in dimensionless form, becomes

$$\frac{d\hat{u}^{\mathrm{Ca}}}{d\hat{y}} = \begin{cases} \hat{\kappa}\left[\hat{\tau} - 2\hat{\tau}_0^{1/2}\hat{\tau}^{1/2} + \hat{\tau}_0\right] & \text{for } \hat{\tau} > \hat{\tau}_0 \\ 0 & \text{for } \hat{\tau} \leq \hat{\tau}_0 \end{cases}, \tag{27}$$

where $\hat{u} = u/u_s$ and $\hat{\tau}_0 = \tau_0/\tau_E$ are the normalized velocity and yield stress. The superscript "Ca" is used to distinguish a velocity of the Casson model.

On using Eqs. (10) and (12) for the stress distribution $\hat{\tau}(\hat{y})$, we may obtain for the sheared region $(0 \leq \hat{y} < \hat{y}_0)$ the velocity satisfying the no-slip wall condition as follows:

$$\hat{u}^{\mathrm{Ca}}(\hat{y}) = 1 - \hat{\psi}(\hat{y}) - 2\left[\hat{\tau}_0\hat{\tau}_w\right]^{1/2} I_2(\hat{y}) + \hat{\tau}_0\hat{\kappa}\,\hat{y}, \tag{28}$$

where $\hat{\psi}(\hat{y})$ and $\hat{\tau}_w$ are given by Eqs. (7) and (13), respectively. The plug-flow velocity in the unsheared region $(\hat{y}_0 < \hat{y} \leq 1)$ is then given by $\hat{u}_p^{\mathrm{Ca}} = \hat{u}^{\mathrm{Ca}}(\hat{y}_0)$, where the yield height $\hat{y}_0$ is given by Eq. (22).

In Eq. (28), I_2 is the following integral:

$$I_2(\hat{y}) = \int_0^{\hat{y}} \frac{\hat{\kappa}\,d\hat{y}}{\sqrt{\cosh^2(\hat{\zeta})e^{\hat{\kappa}\hat{y}} - \sinh^2(\hat{\zeta})e^{-\hat{\kappa}\hat{y}}}}, \tag{29}$$

which does not have a closed-form analytical formula in general. For small zeta potentials such that $\hat{\zeta} < 1$, we may obtain an approximation for I_2, on applying the Taylor and binomial expansions to the integrand, as follows:

$$\begin{aligned} I_2^{\mathrm{app}}(\hat{y}) = {} & 2 - 2e^{-\hat{\kappa}\hat{y}/2} + \left(-\frac{4}{5} - \frac{1}{5}e^{-5\kappa y/2} + e^{-\hat{\kappa}\hat{y}/2}\right)\hat{\zeta}^2 \\ & + \left(\frac{4}{15} - \frac{1}{12}e^{-9\hat{\kappa}\hat{y}/2} + \frac{7}{30}e^{-5\hat{\kappa}\hat{y}/2} - \frac{5}{12}e^{-\hat{\kappa}\hat{y}/2}\right)\hat{\zeta}^4 \\ & + \left(-\frac{88}{975} - \frac{5}{104}e^{-13\hat{\kappa}\hat{y}/2} + \frac{11}{72}e^{-9\hat{\kappa}\hat{y}/2} - \frac{331}{1800}e^{-5\hat{\kappa}\hat{y}/2} + \frac{61}{360}e^{-\hat{\kappa}\hat{y}/2}\right)\hat{\zeta}^6 \end{aligned} \tag{30}$$

with a truncation error of $O(\hat{\zeta}^8)$. The accuracy of I_2^{app} is checked by comparison with the exact values, as shown in Table I. We have found that this approximate formula is accurate for a finite $\hat{\zeta}$ that is as large as $\hat{\zeta} = 0.8$. When $\hat{\zeta} > 0.8$, the integral I_2 has to be evaluated numerically. In this work, Simpson's rule for numerical integration is used.

TABLE I. Comparison between the numerically evaluated exact values of the integral I_2 and the analytical approximation I_2^{app} given by Eq. (30), where $\hat{\kappa} = 100$.

	$\hat{\zeta} = 0.4$		$\hat{\zeta} = 0.6$		$\hat{\zeta} = 0.8$	
$\hat{y}$	I_2^{exact}	I_2^{app}	I_2^{exact}	I_2^{app}	I_2^{exact}	I_2^{app}
0.005	0.00430	0.00430	0.00393	0.00393	0.00414	0.00414
0.01	0.00754	0.00754	0.00665	0.00666	0.00715	0.00716
0.05	0.01727	0.01727	0.01455	0.01452	0.01604	0.01604
0.1	0.01866	0.01866	0.01568	0.01564	0.01731	0.01731
0.5	0.01879	0.01878	0.01578	0.01574	0.01743	0.01742
1.0	0.01879	0.01878	0.01578	0.01574	0.01743	0.01742

In the Newtonian limit, $\hat{\tau}_0 = 0$, Eq. (28) reduces to $\hat{u}(\hat{y}) = 1 - \hat{\psi}(\hat{y})$, which is Eq. (18), as expected. In the limit of a very small zeta potential, Eq. (28) gives

$$\lim_{\hat{\zeta}\to 0} \hat{u}^{\mathrm{Ca}}(\hat{y}) = 1 - e^{-\hat{\kappa}\hat{y}} - 4\hat{\tau}_0^{1/2}\left(1 - e^{-\hat{\kappa}\hat{y}/2}\right) + \hat{\tau}_0\hat{\kappa}\hat{y} \qquad \text{in } 0 \le \hat{y} < \hat{y}_0. \tag{31}$$

Therefore, on applying Eq. (23), the plug-flow velocity of a Casson fluid under the condition of a very small zeta potential is

$$\lim_{\hat{\zeta}\to 0} \hat{u}_p^{\mathrm{Ca}} = 1 - 4\hat{\tau}_0^{1/2} + \hat{\tau}_0\left[3 - \ln\left(\hat{\tau}_0\right)\right] \qquad \text{in } \hat{y}_0 < \hat{y} \le 1. \tag{32}$$

This limiting velocity profile agrees with the one deduced by Ng[29] based on the Debye–Hückel approximation. For a very small zeta potential, the plug-flow velocity of a Casson fluid is decreased by the yield stress through a leading term of order $\hat{\tau}_0^{1/2}$.

At the opposite extreme of a very large zeta potential,

$$I_2(\hat{y}_0) \to \frac{(2\hat{\kappa}\hat{y}_0)^{1/2}}{\cosh(\hat{\zeta})} \qquad \text{as } \hat{\zeta} \gg 1, \tag{33}$$

by which we may get the following asymptotic limit for the plug-flow velocity of a Casson fluid

$$\hat{u}_p^{\mathrm{Ca}} \to 1 - \frac{1}{2\hat{\zeta}}\left[\ln\left(4\hat{\zeta}\,\hat{\tau}_0\right) + 3\right] \qquad \text{for } \hat{\zeta} \gg 1 \text{ and } \hat{\tau}_0 = O(1), \tag{34}$$

where Eq. (24) has been used. Hence, under a large zeta potential, the plug-flow velocity is decreased by the yield stress only by a weaker term of order $\ln \hat{\tau}_0$. Also, such decreasing effect due to the yield stress is to diminish with increasing zeta potential according to $\hat{\zeta}^{-1}$.

VI. HERSCHEL–BULKLEY FLUID

The Herschel–Bulkley model[32] is as follows:

$$m|\dot{\gamma}|^{n-1}\dot{\gamma} = \begin{cases} [1 - \tau_0/|\tau|]\,\tau & \text{for } |\tau| > \tau_0 \\ 0 & \text{for } |\tau| \le \tau_0 \end{cases}, \tag{35}$$

where τ is the stress tensor, $\dot{\gamma} = \nabla\mathbf{u} + (\nabla\mathbf{u})^T$ is the rate of deformation tensor, $\tau_0 \ge$ is the yield stress, m is the consistency parameter, n is the flow index, and

$$|\dot{\gamma}| = \sqrt{\tfrac{1}{2}\dot{\gamma} : \dot{\gamma}}, \qquad |\tau| = \sqrt{\tfrac{1}{2}\tau : \tau} \tag{36}$$

are the magnitudes of the deformation rate and stress tensors, respectively. As only shear-thinning fluids are of interest here, the flow index in the range $0 < n < 1$ is considered. The Herschel–Bulkley model reduces to the power-law model when $\tau_0 = 0$, and to the Bingham model when $n = 1$.

Under simple shear, the Herschel–Bulkley model, in dimensionless form, can be written as

$$\frac{d\hat{u}_n^{\mathrm{HB}}}{d\hat{y}} = \begin{cases} \frac{\hat{\kappa}}{n}\left(\hat{\tau} - \hat{\tau}_0\right)^{1/n} & \text{for } \hat{\tau} > \hat{\tau}_0 \\ 0 & \text{for } \hat{\tau} \le \hat{\tau}_0 \end{cases}, \tag{37}$$

where $\hat{u}_n = u_n/u_{sn}$, $(\hat{\tau},\ \hat{\tau}_0) = (\tau,\ \tau_0)/\tau_E$ are the normalized velocity and stress. The superscript "HB" and subscript "n" are used to denote a velocity of Herschel–Bulkley fluid of flow index n. The generalized Smoluchowski velocity for a power-law fluid[7,12] is used here to normalize the velocity

$$u_{sn} = \frac{n}{\kappa}\left(\frac{\tau_E}{m}\right)^{1/n} = n\kappa^{(1-n)/n}\left(-\frac{\epsilon\zeta E_x}{m}\right)^{1/n}. \tag{38}$$

Obviously, when $n = 1$ and $m = \mu$, the generalized Smoluchowski velocity reduces to the Newtonian Smoluchowski velocity given in Eq. (17), or $u_{s1} = u_s$.

Upon substitution of Eq. (12), Eq. (37) can be integrated with respect to $\hat{y}$ to yield the velocity profile. In the sheared region ($0 \le \hat{y} < \hat{y}_0$):

$$\hat{u}_n^{\mathrm{HB}}(\hat{y}) = \frac{\hat{\kappa}}{n}\int_0^{\hat{y}} \left(\frac{\hat{\tau}_w}{\cosh^2(\hat{\zeta})e^{\hat{\kappa}\hat{y}} - \sinh^2(\hat{\zeta})e^{-\hat{\kappa}\hat{y}}} - \hat{\tau}_0 \right)^{1/n} d\hat{y}, \tag{39}$$

where $\hat{\tau}_w$ is given in Eq. (13). The plug-flow velocity in the unsheared region ($\hat{y}_0 < \hat{y} \le 1$) is then given by $\hat{u}_{pn}^{\mathrm{HB}} = \hat{u}_n^{\mathrm{HB}}(\hat{y}_0)$, where the yield height $\hat{y}_0$ is given by Eq. (22).

For $\hat{\tau}_0 \neq 0$, the integral in Eq. (39) does not have a closed-form formula in general. It can be analytically evaluated, however, when n is the reciprocal of an integer. The largest four such values of the flow index: $n = 1/2, 1/3, 1/4, 1/5$ are considered here. The velocity profiles in the sheared region ($0 \le \hat{y} < \hat{y}_0$) for these selected values of n are given as follows:

$$\hat{u}_{1/2}^{\mathrm{HB}}(\hat{y}) = 2\hat{\tau}_w^2 I_{1/2}(\hat{y}) - 4\hat{\tau}_0\left[1 - \hat{\psi}(\hat{y})\right] + 2\hat{\tau}_0^2\hat{\kappa}\hat{y}, \tag{40}$$

$$\hat{u}_{1/3}^{\mathrm{HB}}(\hat{y}) = 3\hat{\tau}_w^3 I_{1/3}(\hat{y}) - 9\hat{\tau}_0\hat{\tau}_w^2 I_{1/2}(\hat{y}) + 9\hat{\tau}_0^2\left[1 - \hat{\psi}(\hat{y})\right] - 3\hat{\tau}_0^3\hat{\kappa}\hat{y}, \tag{41}$$

$$\begin{aligned}\hat{u}_{1/4}^{\mathrm{HB}}(\hat{y}) = {} & 4\hat{\tau}_w^4 I_{1/4}(\hat{y}) - 16\hat{\tau}_0\hat{\tau}_w^3 I_{1/3}(\hat{y}) + 24\hat{\tau}_0^2\hat{\tau}_w^2 I_{1/2}(\hat{y}) \\ & - 16\hat{\tau}_0^3\left[1 - \hat{\psi}(\hat{y})\right] + 4\hat{\tau}_0^4\hat{\kappa}\hat{y},\end{aligned} \tag{42}$$

$$\begin{aligned}\hat{u}_{1/5}^{\mathrm{HB}}(\hat{y}) = {} & 5\hat{\tau}_w^5 I_{1/5}(\hat{y}) - 25\hat{\tau}_0\hat{\tau}_w^4 I_{1/4}(\hat{y}) + 50\hat{\tau}_0^2\hat{\tau}_w^3 I_{1/3}(\hat{y}) \\ & - 50\hat{\tau}_0^3\hat{\tau}_w^2 I_{1/2}(\hat{y}) + 25\hat{\tau}_0^4\left[1 - \hat{\psi}(\hat{y})\right] - 5\hat{\tau}_0^5\hat{\kappa}\hat{y},\end{aligned} \tag{43}$$

where $\hat{\psi}(\hat{y})$ and $\hat{\tau}_w$ are, respectively, given by Eqs. (7) and (13),

$$\begin{aligned}I_{1/2}(\hat{y}) &= \int_0^{\hat{y}} \frac{\hat{\kappa}\,d\hat{y}}{\left[\cosh^2(\hat{\zeta})e^{\kappa y} - \sinh^2(\hat{\zeta})e^{-\kappa y}\right]^2} \\ &= \frac{2e^{-2\hat{\kappa}\hat{y}}}{\sinh^2(2\hat{\zeta})\left[e^{-2\hat{\kappa}\hat{y}} - \coth^2(\hat{\zeta})\right]} + \frac{1}{2\cosh^2(\hat{\zeta})},\end{aligned} \tag{44}$$

$$\begin{aligned}I_{1/3}(\hat{y}) &= \int_0^{\hat{y}} \frac{\hat{\kappa}\,d\hat{y}}{\left[\cosh^2(\hat{\zeta})e^{\hat{\kappa}\hat{y}} - \sinh^2(\hat{\zeta})e^{-\hat{\kappa}\hat{y}}\right]^3} \\ &= -\frac{\cosh^2(\hat{\zeta})e^{\hat{\kappa}\hat{y}} + \sinh^2(\hat{\zeta})e^{-\hat{\kappa}\hat{y}}}{2\sinh^2(2\hat{\zeta})\left[\cosh^2(\hat{\zeta})e^{\hat{\kappa}\hat{y}} - \sinh^2(\hat{\zeta})e^{-\hat{\kappa}\hat{y}}\right]^2} + \frac{\ln\left[\frac{1+\tanh(\hat{\zeta})e^{-\hat{\kappa}\hat{y}}}{1-\tanh(\hat{\zeta})e^{-\hat{\kappa}\hat{y}}}\right]}{2\sinh^3(2\hat{\zeta})} \\ &\quad + \frac{\cosh(2\hat{\zeta})}{2\sinh^2(2\hat{\zeta})} - \frac{\hat{\zeta}}{\sinh^3(2\hat{\zeta})},\end{aligned} \tag{45}$$

$$\begin{aligned}I_{1/4}(\hat{y}) &= \int_0^{\hat{y}} \frac{\hat{\kappa}\,d\hat{y}}{\left[\cosh^2(\hat{\zeta})e^{\hat{\kappa}\hat{y}} - \sinh^2(\hat{\zeta})e^{-\hat{\kappa}\hat{y}}\right]^4} \\ &= -\frac{1 + 3e^{2\hat{\kappa}\hat{y}} - \left(1 - 3e^{2\hat{\kappa}\hat{y}}\right)\cosh(2\hat{\zeta})}{3\left[1 + e^{2\hat{\kappa}\hat{y}} - \left(1 - e^{2\hat{\kappa}\hat{y}}\right)\cosh(2\hat{\zeta})\right]^3\cosh^4(\hat{\zeta})} + \frac{2 + \cosh(2\hat{\zeta})}{12\cosh^4(\hat{\zeta})},\end{aligned} \tag{46}$$

$$I_{1/5}(\hat{y}) = \int_0^{\hat{y}} \frac{\hat{\kappa}\, d\hat{y}}{\left[\cosh^2(\hat{\zeta}) e^{\hat{\kappa}\hat{y}} - \sinh^2(\hat{\zeta}) e^{-\hat{\kappa}\hat{y}}\right]^5}$$

$$= \frac{e^{-\hat{\kappa}\hat{y}}\left[\cosh^2(\hat{\zeta}) + \sinh^2(\hat{\zeta}) e^{-2\hat{\kappa}\hat{y}}\right]}{8\sinh^4(2\hat{\zeta})\left[\cosh^2(\hat{\zeta}) - \sinh^2(\hat{\zeta}) e^{-2\hat{\kappa}\hat{y}}\right]^4}$$

$$\times \left[3\sinh^4(\hat{\zeta}) e^{-4\hat{\kappa}\hat{y}} - 14\cosh^2(\hat{\zeta})\sinh^2(\hat{\zeta}) e^{-2\hat{\kappa}\hat{y}} + 3\cosh^4(\hat{\zeta})\right]$$

$$- \frac{3\ln\left[\frac{1+\tanh(\hat{\zeta}) e^{-\hat{\kappa}\hat{y}}}{1-\tanh(\hat{\zeta}) e^{-\hat{\kappa}\hat{y}}}\right]}{8\sinh^5(2\hat{\zeta})} - \frac{\cosh(2\hat{\zeta})\left[4 - \cosh(4\hat{\zeta})\right]}{8\sinh^4(2\hat{\zeta})} + \frac{3\hat{\zeta}}{4\sinh^5(2\hat{\zeta})}. \tag{47}$$

For other values of n than those equal to the reciprocal of an integer, we may evaluate Eq. (39) by numerical integration using Simpson's rule.

In the limit of a very small zeta potential $\hat{\zeta} \to 0$, the integrals above are simply given by

$$\lim_{\hat{\zeta}\to 0} I_n(\hat{y}) = n\left(1 - e^{-\hat{\kappa}\hat{y}/n}\right). \tag{48}$$

Hence, by using Eqs. (19) and (23), the plug-flow velocities for a very small zeta potential are readily obtained as follows:

$$\lim_{\hat{\zeta}\to 0} \hat{u}^{\mathrm{HB}}_{p(1/2)} = 1 - 4\hat{\tau}_0 + \hat{\tau}_0^2\left[3 - 2\ln(\hat{\tau}_0)\right], \tag{49}$$

$$\lim_{\hat{\zeta}\to 0} \hat{u}^{\mathrm{HB}}_{p(1/3)} = 1 - \frac{9}{2}\hat{\tau}_0 + 9\hat{\tau}_0^2 + \hat{\tau}_0^3\left[-\frac{11}{2} + 3\ln(\hat{\tau}_0)\right], \tag{50}$$

$$\lim_{\hat{\zeta}\to 0} \hat{u}^{\mathrm{HB}}_{p(1/4)} = 1 - \frac{16}{3}\hat{\tau}_0 + 12\hat{\tau}_0^2 - 16\hat{\tau}_0^3 + \hat{\tau}_0^4\left[\frac{25}{3} - 4\ln(\hat{\tau}_0)\right], \tag{51}$$

$$\lim_{\hat{\zeta}\to 0} \hat{u}^{\mathrm{HB}}_{p(1/5)} = 1 - \frac{25}{4}\hat{\tau}_0 + \frac{50}{3}\hat{\tau}_0^2 - 25\hat{\tau}_0^3 + 25\hat{\tau}_0^4 + \hat{\tau}_0^5\left[-\frac{137}{12} + 5\ln(\hat{\tau}_0)\right], \tag{52}$$

where $\hat{\tau}_0 < 1$. For a very small zeta potential, the plug-flow velocity of a Herschel–Bulkley fluid is decreased by the yield stress through a leading term of order $\hat{\tau}_0$ for all values of n considered here.

At the other extreme, for a very large zeta potential ($\hat{\zeta} \gg 1$), the plug-flow velocities will tend to the following asymptotic limits:

$$\hat{u}^{\mathrm{HB}}_{p(1/2)} \to \frac{\cosh^2(\hat{\zeta})}{\hat{\zeta}^2} - 4\hat{\tau}_0\left[1 - \frac{1}{2\hat{\zeta}}\ln\left(4\hat{\zeta}\hat{\tau}_0\right)\right] + \cdots, \tag{53}$$

$$\hat{u}^{\mathrm{HB}}_{p(1/3)} \to \frac{3\cosh^4(\hat{\zeta})}{4\hat{\zeta}^3} - \frac{9\cosh^2(\hat{\zeta})}{2\hat{\zeta}^2}\hat{\tau}_0 + \cdots, \tag{54}$$

$$\hat{u}^{\mathrm{HB}}_{p(1/4)} \to \frac{2\cosh^6(\hat{\zeta})}{3\hat{\zeta}^4} - \frac{4\cosh^4(\hat{\zeta})}{\hat{\zeta}^3}\hat{\tau}_0 + \cdots, \tag{55}$$

$$\hat{u}^{\mathrm{HB}}_{p(1/5)} \to \frac{5\cosh^8(\hat{\zeta})}{8\hat{\zeta}^5} - \frac{25\cosh^6(\hat{\zeta})}{6\hat{\zeta}^4}\hat{\tau}_0 + \cdots, \tag{56}$$

where only the leading terms are shown in each limit above. Remarkably, these velocities will increase exponentially with the zeta potential, where the exponential growth is faster for smaller n. The terms associated with the yield stress are subdominant, and hence the effect due to a finite yield stress is always negligible under the condition $\hat{\zeta} \gg 1$ for a Herschel–Bulkley fluid with $n < 1$.

A. Power-law fluid

When the yield stress is zero, $\hat{\tau}_0 = 0$, the Herschel–Bulkley model reduces to the power-law model, for which the problem has been previously studied by Zhao and Yang.[12] The integral in Eq. (39) without $\hat{\tau}_0$ can be analytically expressed as follows:

$$\hat{u}_n^{\mathrm{PL}}(\hat{y}) = \frac{\hat{\kappa}}{n}\int_0^{\hat{y}} \frac{\hat{\tau}_w^{1/n} d\hat{y}}{\left[\cosh^2(\hat{\zeta})e^{\hat{\kappa}\hat{y}} - \sinh^2(\hat{\zeta})e^{-\hat{\kappa}\hat{y}}\right]^{1/n}}$$
$$= \hat{\tau}_w^{1/n}\left[H\left(\hat{\kappa}\hat{y}, n\right) - H\left(0, n\right)\right] \qquad \text{for } \hat{\tau}_0 = 0, \tag{57}$$

where the superscript "PL" is used to denote the case of power-law model, and

$$H(\hat{\kappa}\hat{y}, n) = \left(-\frac{e^{\hat{\kappa}\hat{y}}}{\sinh^2(\hat{\zeta})}\right)^{1/n} {}_2F_1\left(\frac{1}{2n}, \frac{1}{n}; \frac{1+2n}{2n}; e^{2\hat{\kappa}\hat{y}}\coth^2(\hat{\zeta})\right), \tag{58}$$

in which ${}_2F_1(a, b; c; z)$ is the Gauss hypergeometric function. Without a yield stress, the plug-flow velocity is the asymptotic limit of the velocity far outside the EDL, which is analytically given by

$$\hat{u}_{pn}^{\mathrm{PL}} = \hat{u}_n^{\mathrm{PL}}(\infty)$$
$$= \left(\frac{\hat{\tau}_w}{\cosh^2(\hat{\zeta})}\right)^{1/n} {}_2F_1\left(\frac{1}{2n}, \frac{1}{n}; \frac{1+2n}{2n}; \tanh^2(\hat{\zeta})\right) \qquad \text{for } \hat{\tau}_0 = 0. \tag{59}$$

Zhao and Yang[12] are the first who derived the power-law EO flow profiles in terms of the hypergeometric functions. We have obtained Eqs. (57)–(59) using *Mathematica*® 9.0. The special cases of Eq. (59) in the limits of Newtonian fluid, small and large $\hat{\zeta}$ have been discussed by Zhao and Yang.[12]

For $n = 1/2, 1/3, 1/4, 1/5$, the hypergeometric function in Eq. (59) is expressible by elementary functions, which can be readily found with *Mathematica*.® The plug-flow velocities for power-law fluids with these values of n are as follows:

$$\hat{u}_{p(1/2)}^{\mathrm{PL}} = \frac{\hat{\tau}_w^2}{\cosh^2(\hat{\zeta})}, \tag{60}$$

$$\hat{u}_{p(1/3)}^{\mathrm{PL}} = 3\hat{\tau}_w^3\left[\frac{\cosh(2\hat{\zeta})}{2\sinh^2(2\hat{\zeta})} - \frac{\hat{\zeta}}{\sinh^3(2\hat{\zeta})}\right], \tag{61}$$

$$\hat{u}_{p(1/4)}^{\mathrm{PL}} = \hat{\tau}_w^4\left[\frac{2+\cosh(2\hat{\zeta})}{3\cosh^4(\hat{\zeta})}\right], \tag{62}$$

$$\hat{u}_{p(1/5)}^{\mathrm{PL}} = 5\hat{\tau}_w^5\left\{\frac{\cosh(2\hat{\zeta})\left[\cosh(4\hat{\zeta}) - 4\right]}{8\sinh^4(2\hat{\zeta})} + \frac{3\hat{\zeta}}{4\sinh^5(2\hat{\zeta})}\right\}, \tag{63}$$

which can be checked to agree with the far-from-wall limits given by Eqs. (40)–(47) on omitting terms containing $\hat{\tau}_0$ in these equations. Also, it is easy to prove that all these velocities tend to the limit of 1 when $\hat{\zeta} \to 0$. The leading terms of these velocities can also be checked to agree with those of Eqs. (53)–(56) when $\hat{\zeta} \gg 1$, for which the velocities will blow up exponentially, where the rate of exponential growth is higher for smaller n.

VII. BINGHAM PLASTIC

Bingham plastic is a Herschel–Bulkley fluid with a unity flow index, $n = 1$, for which the consistency parameter can be replaced by the plastic viscosity, $m = \mu$. Under simple shear, the Bingham model, in dimensionless form, reads

$$\frac{d\hat{u}^{\mathrm{Bn}}}{d\hat{y}} = \begin{cases} \hat{\kappa}\left(\hat{\tau} - \hat{\tau}_0\right) & \text{for } \hat{\tau} > \hat{\tau}_0 \\ 0 & \text{for } \hat{\tau} \le \hat{\tau}_0 \end{cases}, \tag{64}$$

where $\hat{u} = u/u_s$, $(\hat{\tau},\ \hat{\tau}_0) = (\tau,\ \tau_0)/\tau_E$ are the normalized velocity and stress. The superscript "Bn" is used to distinguish a velocity of the Bingham model.

On using Eqs. (10) and (12) for the stress distribution $\hat{\tau}(\hat{y})$, we may obtain for the sheared region $(0 \le \hat{y} < \hat{y}_0)$ the velocity satisfying the no-slip wall condition as follows:

$$\hat{u}^{\mathrm{Bn}}(\hat{y}) = 1 - \hat{\psi}(\hat{y}) - \hat{\tau}_0 \hat{\kappa}\, \hat{y}, \tag{65}$$

where $\hat{\psi}(\hat{y})$ is given by Eq. (7). The plug-flow velocity in the unsheared region $(\hat{y}_0 < \hat{y} \le 1)$ is then given by $\hat{u}_p^{\mathrm{Bn}} = \hat{u}^{\mathrm{Bn}}(\hat{y}_0) = 1 - \hat{\psi}(\hat{y}_0) - \hat{\tau}_0 \hat{\kappa}\, \hat{y}_0$, where the yield height $\hat{y}_0$ is given by Eq. (22).

In the Newtonian limit, $\hat{\tau}_0 = 0$, Eq. (65) reduces to $\hat{u}(\hat{y}) = 1 - \hat{\psi}(\hat{y})$, which is Eq. (18), as expected. In the limit of a small zeta potential, Eq. (65) gives

$$\lim_{\hat{\zeta}\to 0} \hat{u}^{\mathrm{Bn}}(\hat{y}) = 1 - e^{-\hat{\kappa}\hat{y}} - \hat{\tau}_0 \hat{\kappa}\, \hat{y} \qquad \text{in } 0 \le \hat{y} < \hat{y}_0. \tag{66}$$

Therefore, on applying Eq. (23), the plug-flow velocity in this limit is given by

$$\lim_{\hat{\zeta}\to 0} \hat{u}_p^{\mathrm{Bn}} = 1 + \hat{\tau}_0 \left[\ln(\hat{\tau}_0) - 1\right] \qquad \text{in } \hat{y}_0 < \hat{y} \le 1. \tag{67}$$

For a very small zeta potential, the plug-flow velocity of a Bingham plastic is decreased by the yield stress according to terms of linear order of $\hat{\tau}_0$, which is similar to that for a Herschel–Bulkley fluid with $n < 1$.

At the other extreme, for a very large zeta potential, the plug-flow velocity of a Bingham plastic tends to the following asymptotic limit:

$$\hat{u}_p^{\mathrm{Bn}} \to 1 - \frac{1}{2\hat{\zeta}} \left[\ln\left(4\hat{\zeta}\,\hat{\tau}_0\right) + 1\right] \qquad \text{for } \hat{\zeta} \gg 1 \text{ and } \hat{\tau}_0 = O(1), \tag{68}$$

where Eq. (24) has been used. Hence, unlike a Herschel–Bulkley fluid with $n < 1$, the plug-flow velocity $\hat{u}_p$ of a Bingham plastic $(n = 1)$ will not blow up exponentially, but instead is upper-bounded by 1, as $\hat{\zeta}$ becomes very large. We further note that Eq. (68) is similar in form to Eq. (34), which is the counterpart large-$\hat{\zeta}$ asymptote for a Casson fluid. Bingham plastics and Casson fluids will have similar dependence on the yield stress and zeta potential, when the zeta potential becomes very large. In this asymptotic limit, the plug-flow velocity is decreased by the yield stress only through a weaker term of order $\ln \hat{\tau}_0$. On the other hand, such decreasing effect of the yield stress will diminish algebraically according to $\hat{\zeta}^{-1}$.

VIII. RESULTS AND DISCUSSIONS

A. Casson fluid

We show in Figs. 4(a) and 4(b), for Casson fluids, the plug-flow velocity $\hat{u}_p$ as a function of the yield stress $\hat{\tau}_0$ and zeta potential $\hat{\zeta}$. We first recall that, as has been shown in Fig. 3, the yield height $\hat{y}_0$ decreases when either the yield stress $\hat{\tau}_0$ or the zeta potential $\hat{\zeta}$ increases. Here, when $\hat{\tau}_0$ increases, as shown in Fig. 4(a), the plug-flow velocity decreases. However, when $\hat{\zeta}$ increases, as shown in Fig. 4(b), the plug-flow velocity increases. In the former case, a larger yield stress results in a smaller yield height, thereby a smaller plug-flow velocity, as reasoned earlier. In the latter case, a larger zeta potential gives rise to a stronger stress distribution. Although the sheared region is reduced in height, the larger stress in the sheared region leads to a larger plug-flow velocity in the unsheared region.

For a Casson fluid, the plug-flow velocity can be sensitively decreased by the yield stress for sufficiently small zeta potential; see Fig. 4(b). A yield stress as small as $\hat{\tau}_0 = 0.001$ can decrease $\hat{u}_p$ by more than 10% when $\hat{\zeta} \le 1$. For a very large zeta potential, say $\hat{\zeta} \ge 100$, the plug-flow velocity becomes much less sensitively affected by the yield stress. This can be illustrated by a yield stress of $\hat{\tau}_0 = 0.8$, which will decrease $\hat{u}_p$ by more than 99.9% when $\hat{\zeta} < 0.1$, but in sharp contrast by only 5% or smaller when $\hat{\zeta} > 100$. From Fig. 4(b), we also see that the $\hat{\zeta} \to 0$ limit of $\hat{u}_p$, given by Eq. (32), can be practically attained when $\hat{\zeta} \le O(0.1)$.

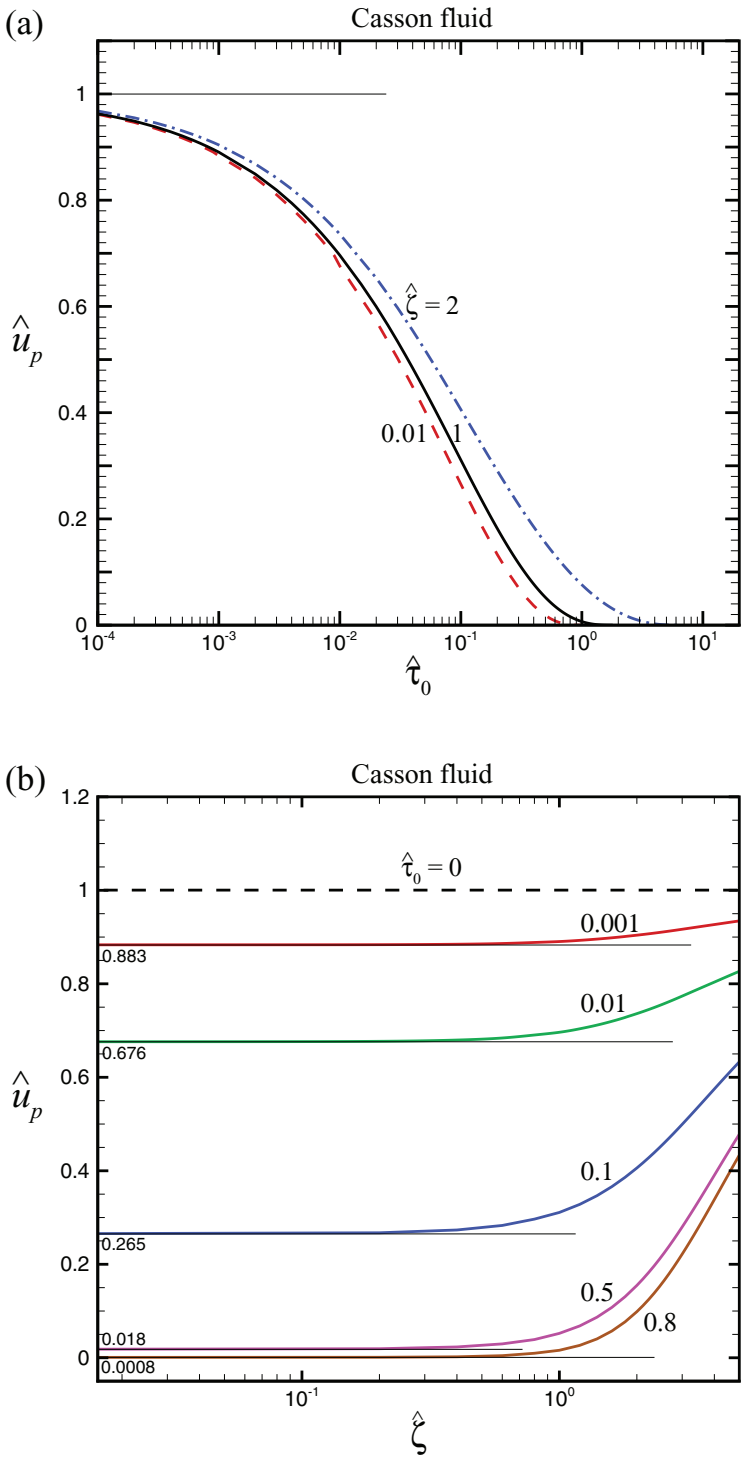

FIG. 4. For Casson fluids, the normalized plug-flow velocity $\hat{u}_p$ as a function of (a) normalized yield stress $\hat{\tau}_0$ for several values of $\hat{\zeta}$, and (b) normalized zeta potential $\hat{\zeta}$ for several values of $\hat{\tau}_0$, where $\hat{\kappa} = 100$. The asymptotic limits for $\hat{\zeta} \to 0$, which are computed by Eq. (32), are shown on the left end of curves shown in (b).

B. Herschel–Bulkley fluid and Bingham plastic

We show in Figs. 5(a) and 5(b), for Herschel–Bulkley fluids (including Bingham plastic), the plug-flow velocity $\hat{u}_{pn}$ as a function of the yield stress $\hat{\tau}_0$ for zeta potential $\hat{\zeta} = 0.01,\ 1$. Based on

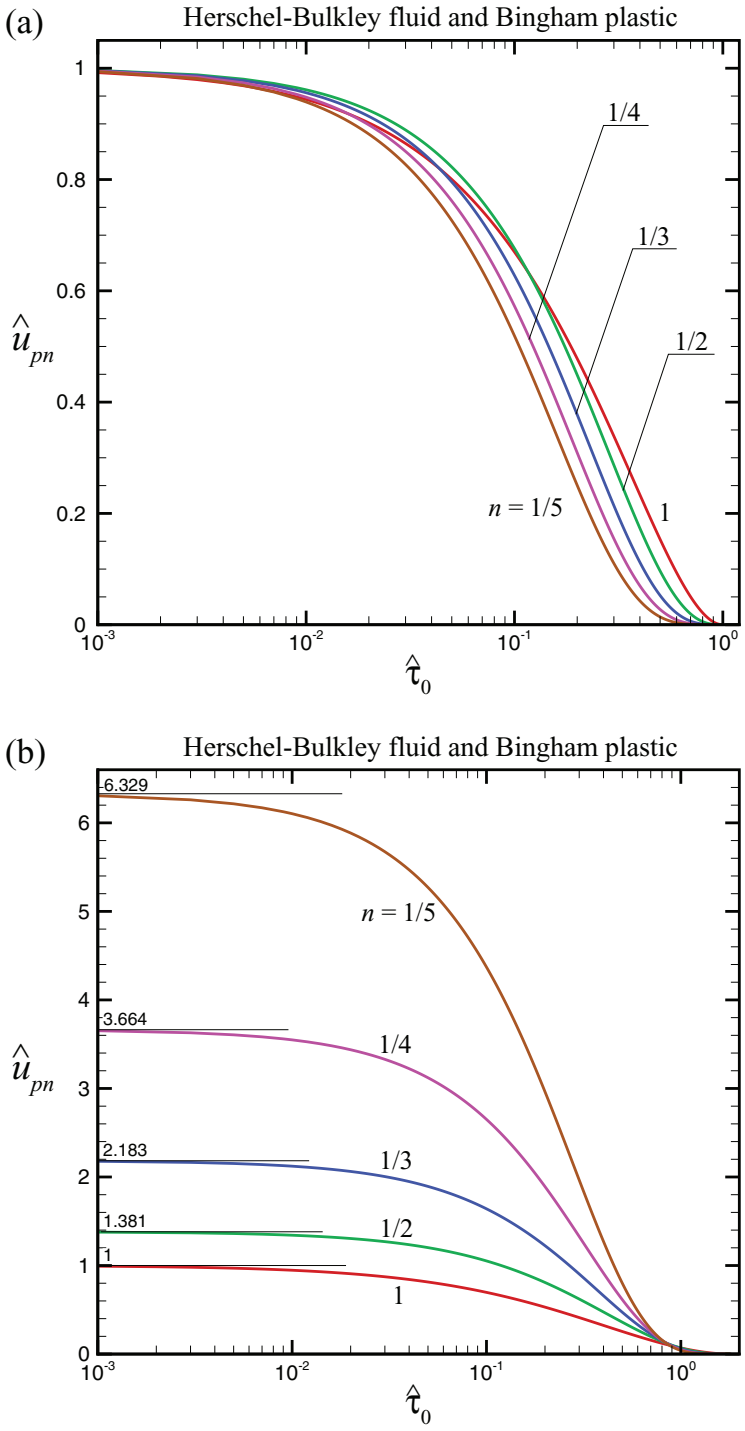

FIG. 5. For Herschel–Bulkley fluid, the normalized plug-flow velocity $\hat{u}_{pn}$ as a function of the normalized yield stress $\hat{\tau}_0$ for some values of n, and (a) $\hat{\zeta} = 0.01$, (b) $\hat{\zeta} = 1$, where $\hat{\kappa} = 100$. The asymptotic limits for $\hat{\tau}_0 \to 0$ (i.e., power-law fluid), which are computed by Eqs. (60)–(63), are shown on the left end of curves in (b).

these figures, the following observations can be made. First, $\hat{u}_{pn}$ is not appreciably lowered by the yield stress unless $\hat{\tau}_0 \geq O(0.01)$. Recall that for a Casson fluid the plug-flow velocity is already decreased by more than 30% by this order of the yield stress. When the yield stress is moderately large, say $\hat{\tau}_0 = 0.1$, the plug-flow velocity of a Herschel–Bulkley fluid is decreased only by some

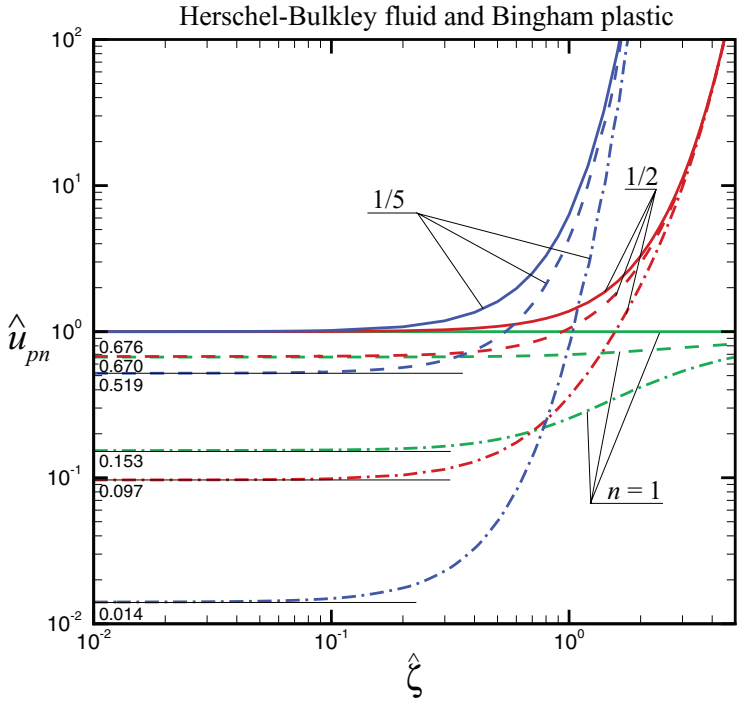

FIG. 6. For Herschel–Bulkley fluid, the normalized plug-flow velocity $\hat{u}_{pn}$ as a function of the normalized zeta potential $\hat{\zeta}$ for $n = 1$(Binghamplastic), 1/2, 1/5, where $\hat{\kappa} = 100$, and $\hat{\tau}_0 = 0$ (solid lines), $\hat{\tau}_0 = 0.1$ (dashed lines), $\hat{\tau}_0 = 0.5$ (dashed-dotted lines). The asymptotic limits for $\hat{\zeta} \to 0$, which are computed by Eqs. (49), (52), and (67), are shown on the left end of curves.

30%, while that of a Casson fluid is already decreased by some 70%. Hence, we may conclude that a Herschel–Bulkley fluid (including Bingham plastic) is in general not as strongly affected by the yield stress as a Casson fluid for the reduction of the plug-flow velocity by the yield stress. Second, for a zeta potential as small as $\hat{\zeta} = O(0.01)$, a smaller flow index n tends to have a larger decreasing effect due to the yield stress on the plug-flow velocity. The effect may, however, vary non-monotonically with n, depending on $\hat{\tau}_0$ and $\hat{\zeta}$. Anyway, for a zeta potential that is smaller than order unity, the flow index n has a relatively mild effect in the problem. Changing n, within the range of values studied, will not significantly change how the yield stress affects the plug-flow velocity.

For a zeta potential that is order unity or larger, the flow index n can have a much more dramatic effect in the problem. We show in Fig. 6 the plug-flow velocity as a function of the zeta potential for $n = 1$ (Bingham plastic) and $n = 1/2, 1/5$. For $n = 1$, a non-zero yield stress will continue to have a finite, although reduced, effect on the plug-flow velocity when the zeta potential becomes larger than order unity. For $n < 1$, increasing the zeta potential beyond order unity will cause the plug-flow velocity to blow up exponentially, whether the yield stress being zero or not. Consequently, a finite yield stress, $\hat{\tau}_0 = O(1)$, will quickly lose its influence on the plug-flow velocity as the flow index drops below unity, $n < 1$, when the zeta potential is larger than order unity, $\hat{\zeta} \gg 1$.

C. Comparison between the models

To summarize our discussions presented above, and to further illustrate the effect of yield stress on the plug-flow velocity for different materials, we present in Table II some representative values of the following quantity:

$$\Delta\hat{u}_p(\hat{\tau}_0) = \frac{\hat{u}_p(\text{without yield stress}) - \hat{u}_p(\hat{\tau}_0)}{\hat{u}_p(\text{without yield stress})} \times 100\%, \tag{69}$$

TABLE II. The percentage reduction of the plug-flow velocity under the effect of yield stress for different viscoplastic materials. In columns 3–9, the values are $\Delta\hat{u}_p$, defined in Eq. (69), where $\hat{\kappa} = 100$. Bingham plastic amounts to $n = 1$ of Herschel–Bulkley fluid.

		Casson	Bingham	Herschel–Bulkley fluid				
$\hat{\zeta}$	$\hat{\tau}_0$	fluid	plastic	$n = 0.9$	$n = 0.75$	$n = 1/2$	$n = 1/3$	$n = 1/5$
0.1	0.01	32.37	5.60	4.99	4.29	3.87	4.39	6.05
	0.1	73.41	32.99	32.13	31.27	32.29	37.09	47.90
	0.5	98.16	84.53	85.04	86.26	90.19	94.62	98.54
1	0.01	30.37	5.33	4.59	3.69	2.81	2.81	3.56
	0.1	68.91	30.34	28.68	26.37	23.85	24.87	30.94
	0.5	94.78	74.52	73.87	73.16	73.94	78.38	87.36
2	0.01	26.38	4.88	3.88	2.61	1.18	0.85	0.97
	0.1	59.40	25.86	22.64	17.65	10.29	8.06	9.35
	0.5	84.52	58.32	54.53	48.01	36.81	33.68	39.47

where $\hat{u}_p$ (without yield stress) is under the same conditions as $\hat{u}_p(\hat{\tau}_0)$ except that the yield stress is zero. This quantity is the percentage reduction of the plug-flow velocity due to the yield stress of the material.

The following points are noted again as a summary to the present study.

1. Among the three kinds of viscoplastic materials that have been examined, a Casson fluid is most sensitive to having its plug-flow velocity be reduced by the yield stress of the material.
2. For any material, the flow is more susceptible to the effect of a yield stress for a lower zeta potential.
3. The small-zeta-potential limit, namely the Debye–Hückel approximation, can remain practically applicable up to $\hat{\zeta} = O(0.1)$ for Casson, Bingham, and Herschel–Bulkley fluids. In this limit, the plug-flow velocity is decreased by the yield stress through a term of order $\hat{\tau}_0^{1/2}$ for Casson fluids, but of order $\hat{\tau}_0$ for Herschel–Bulkley fluids and Bingham plastics.
4. For a small zeta potential such that $\hat{\zeta} < O(1)$, a flow index equal to 1 or smaller than 1 gives rise to comparable effect. Hence, a Bingham plastic behaves not significantly different from a Herschel–Bulkley fluid under a small zeta potential. This is not true for $\hat{\zeta} \geq O(1)$.
5. Increasing the zeta potential to order unity or above can considerably diminish the decreasing effect of a yield stress on the plug-flow velocity. The change due to an increasing zeta potential is relatively mild (algebraically) for a Casson fluid and a Bingham plastic, through a term of order $\hat{\zeta}^{-1}$. In sharp contrast, the change can be very dramatic for a flow index $n < 1$, for which the velocity will blow up as an exponential function of the zeta potential irrespective of the yield stress.

IX. CONCLUDING REMARKS

In this paper, we have developed solutions for EO flow of three types of yield-stress materials, namely, Casson, Herschel–Bulkley, and Bingham fluids, in a slit microchannel without the Debye–Hückel approximation. Analytical expressions are deduced for the plug-flow velocities under the limiting conditions of very small and very large zeta potentials. These analytical limits reveal the different asymptotic behaviors that are exhibited by the different materials. The yield stress is to reduce the Smoluchowski slip velocity, where the reduction of EO velocity is a function of not only the yield stress $\hat{\tau}_0$ itself, but also the zeta potential $\hat{\zeta}$ and the flow index n. Under a small zeta potential, the velocity reduction by the yield stress is of order $\hat{\tau}_0^{1/2}$ for Casson fluids, and of order $\hat{\tau}_0$ for Bingham plastics and Herschel–Bulkley fluids. Under a large zeta potential, the velocity reduction is of order $\hat{\zeta}^{-1}\ln(\hat{\zeta}\hat{\tau}_0)$ for Casson fluids and Bingham plastics, but is virtually zero for Herschel–Bulkley fluids with $n < 1$.

We have for simplicity ignored pressure forcing in the problem. Owing to nonlinearity, adding a forcing to the flow can non-trivially modify the effect due to the yield stress. It is worth pursuing

in a future study an extension of the present theory to determine how various combinations of mechanical and electric forcings will give rise to different dependence of the flow on the rheological parameters.

EO flow of complex fluids is fraught with many open questions. If the complexity of the fluid is due to dispersed inclusions, it is possible that the electric field distribution may change within the Debye layer arising from the inhomogeneity of the inclusions. Whether inhomogeneity of the electric permeability is a pertinent effect in a complex fluid near walls in EO flows needs to be further understood. Future studies should find out more about the interaction between large inclusions and the EDL.

ACKNOWLEDGMENTS

Comments by the reviewers are gratefully acknowledged. The final concluding remark was due to a comment by one of the reviewers. The work was financially supported by the Research Grants Council of the Hong Kong Special Administrative Region, China, through Project No. HKU 715510E.

[1] D. Barthès-Biesel, *Microhydrodynamics and Complex Fluids* (CRC Press, Boca Raton, 2012).
[2] J. M. MacInnes, X. Du, and R. W. K. Allen, "Prediction of electrokinetic and pressure flow in a microchannel T-junction," Phys. Fluids **15**, 1992 (2003).
[3] S. Das and S. Chakraborty, "Analytical solutions for velocity, temperature and concentration distribution in electroosmotic microchannel flows of a non-Newtonian bio-fluid," Anal. Chim. Acta **559**, 15 (2006).
[4] W. B. Zimmerman, J. M. Rees, and T. J. Craven, "Rheometry of non-Newtonian electrokinetic flow in a microchannel T-junction," Microfluid. Nanofluid. **2**, 481 (2006).
[5] S. Chakraborty, "Electroosmotically driven capillary transport of typical non-Newtonian biofluids in rectangular microchannels," Anal. Chim. Acta **605**, 175 (2007).
[6] C. L. A. Berli and M. L. Olivares, "Electrokinetic flow of non-Newtonian fluids in microchannels," J. Colloid Interface Sci. **320**, 582 (2008).
[7] C. Zhao, E. Zholkovskij, J. Masliyah, and C. Yang, "Analysis of electroosmotic flow of power-law fluids in a slit microchannel," J. Colloid Interface Sci. **326**, 503 (2008).
[8] R. P. Bharti, D. J. E. Harvie, and M. R. Davidson, "Electroviscous effects in steady fully developed flow of a power-law liquid through a cylindrical microchannel," Int. J. Heat Fluid Flow **30**, 804 (2009).
[9] M. L. Olivares, L. Vera-Candioti, and C. L. A. Berli, "The EOF of polymer solutions," Electrophoresis **30**, 921 (2009).
[10] G. H. Tang, X. F. Li, Y. L. He, and W. Q. Tao, "Electroosmotic flow of non-Newtonian fluid in microchannels," J. Non-Newtonian Fluid Mech. **157**, 133 (2009).
[11] C. Zhao and C. Yang, "Analysis of power-law fluid flow in a microchannel with electrokinetic effects," Int. J. Emerg. Multi. Fluid Sci. **1**, 37–52 (2009).
[12] C. Zhao and C. Yang, "Nonlinear Smoluchowski velocity for electroosmosis of power-law fluids over a surface with arbitrary zeta potentials," Electrophoresis **31**, 973 (2010).
[13] C. Zhao and C. Yang, "An exact solution for electroosmosis of non-Newtonian fluids in microchannels," J. Non-Newtonian Fluid Mech. **166**, 1076 (2011).
[14] C. L. A. Berli, "Output pressure and efficiency of electrokinetic pumping of non-Newtonian fluids," Microfluid. Nanofluid. **8**, 197 (2010).
[15] N. Vasu and S. De, "Electroviscous effects in purely pressure driven flow and stationary plane analysis in electroosmotic flow of power-law fluids in a slit microchannel," Int. J. Eng. Sci. **48**, 1641 (2010).
[16] N. Vasu and S. De, "Electroosmotic flow of power-law fluids at high zeta potentials," Colloids Surf., A **368**, 44 (2010).
[17] A. Babaie, A. Sadeghi, and M. H. Saidi, "Combined electroosmotically and pressure driven flow of power-law fluids in a slit microchannel," J. Non-Newtonian Fluid Mech. **166**, 792 (2011).
[18] M. Hadigol, R. Nosrati, and M. Raisee, "Numerical analysis of mixed electroosmotic/pressure driven flow of power-law fluids in microchannels and micropumps," Colloids Surf., A **374**, 142 (2011).
[19] A. Sadeghi, M. Fattahi, and M. H. Saidi, "An approximate analytical solution for electro-osmotic flow of power-law fluids in a planar microchannel," J. Heat Trans. **133**, 091701 (2011).
[20] C. C. Cho, C. L. Chen, and C. K. Chen, "Electrokinetically-driven non-Newtonian fluid flow in rough microchannel with complex-wavy surface," J. Non-Newtonian Fluid Mech. **173–174**, 13 (2012).
[21] C. C. Cho, C. L. Chen, and C. K. Chen, "Flow characteristics and mixing performance of electrokinetically driven non-Newtonian fluid in contraction–expansion microchannel," Rheol. Acta **51**, 925 (2012).
[22] M. Shamshiri, R. Khazaeli, M. Ashrafizaadeh, and S. Mortazavi, "Electroviscous and thermal effects on non-Newtonian liquid flows through microchannels," J. Non-Newtonian Fluid Mech. **173–174**, 1 (2012).
[23] M. A. Vakili, A. Sadeghi, M. H. Saidi, and A. A. Mozafari, "Electrokinetically driven fluidic transport of power-law fluids in rectangular microchannels," Colloids Surf., A **414**, 440 (2012).
[24] R. B. Bird, G. C. Dai, and B. J. Yarusso, "The rheology and flow of viscoplastic materials," Rev. Chem. Eng. **1**, 1 (1983).
[25] E. W. Merrill, "Rheology of blood," Physiol. Rev. **49**, 863 (1969).
[26] Q. D. Nguyen and D. V. Boger, "Yield stress measurement for concentrated suspensions," J. Rheol. **27**, 321 (1983).

[27] M. Liu, Y. Liu, Q. Guo, and J. Yang, "Modeling of electroosmotic pumping of nonconducting liquids and biofluids by a two-phase flow method," J. Electroanal. Chem. **636**, 86 (2009).
[28] G. H. Tang, P. X. Ye, and W. Q. Tao, "Pressure-driven and electroosmotic non-Newtonian flows through microporous media via lattice Boltzmann method," J. Non-Newtonian Fluid Mech. **165**, 1536 (2010).
[29] C. O. Ng, "Combined pressure-driven and electroosmotic flow of Casson fluid through a slit microchannel," J. Non-Newtonian Fluid Mech. **198**, 1 (2013).
[30] C. Zhao and C. Yang, "Electro-osmotic mobility of non-Newtonian fluids," Biomicrofluidics **5**, 014110 (2011).
[31] N. Casson, "A flow equation for pigment-oil suspensions of the printing ink type," in *Rheology of Disperse Systems*, edited by C. C. Mill (Pergamon, London, 1959), pp. 84–104.
[32] W. H. Herschel and R. Bulkley, "Measurement of consistency as applied to rubber–benzene solutions," Proc. Am. Soc. Test Mater. **26**, 621 (1926).